Paper 41

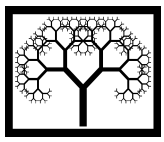


Proceedings of the Eleventh International Conference
on Computational Structures Technology,
B.H.V. Topping, (Editor),
Civil-Comp Press, Stirlingshire, Scotland

# A Two-Node Finite Element for Linear Magneto-Electric Laminated Timoshenko Beams

**A. Milazzo and C. Orlando**
**Dipartimento di Ingegneria Civile Ambientale e Aerospaziale**
**Universitá di Palermo, Italy**

## Abstract

A new finite element is presented for linear magnetoelectric straight laminated beam subject to the assumptions of quasi-steady electromagnetic state. The mechanical model is based upon Timoshenko beam theory to account for shear deformation influences. The electromagnetic stacking sequence is proved to enter the equivalent elastic problem by affecting both the stiffness properties of the beam, in terms of axial and flexural coupling, and by modifying the mechanical boundary conditions as distributed loads. Shape functions are first written for the generalized beam mean-line kinematical quantities in such a way the obtained strain field fulfills the homogeneous governing equations of the equivalent elastic problem. The weak form of the governing equations are then obtained by integrating over the element length the equation of motion of the beam opportunely multiplied by the virtual mean-line axial and transverse displacements and by the virtual cross-sectional rotation. Both the virtual and actual kinematical quantities are then expressed in terms of virtual and actual nodal variables by means of the proposed shape functions. By so doing, the definitions of the element mass and stiffness matrices and of the equivalent force vector are straightforwardly obtained. Lastly, numerical results are presented to assess the soundness of the proposed formulation.

**Keywords:** magnetoelectric laminates, Timoshenko's beam, finite element.

# 1 Introduction

Magneto-electro-elastic composite materials are capable of passively converting energy among the elastic, electric and magnetic forms. They are realized by combining piezoelectric and piezomagnetic materials as constituents in particulate or layered arrangements. [1, 2] The magnetic and the electric fields in such composites

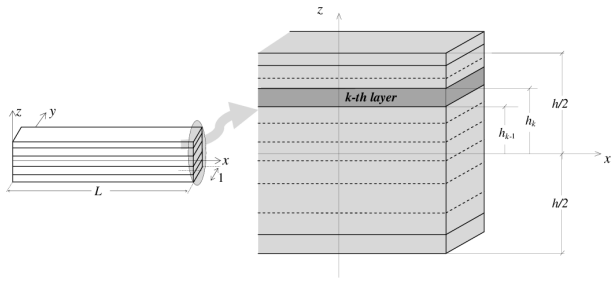


Figure 1: Laminated beam geometrical configuration.

are coupled by mean of elastic deformation [3]. This magneto-electric coupling is a characteristic of the whole composite and it is absent in each phase. The reason for the interest in magneto-electro-elastic composites relies on the wide range of applications they are well suited for, which spans, namely, from magnetic field probes to wireless powering of MEMS as well as to sensors and actuators technology [4, 5, 6, 7]. This has motivated a great number of research papers dealing with the analytical and the numerical structural-like modeling of magneto-electro-elastic composites [8, 9, 10, 11, 12, 13, 14].

In this paper a two-node 1-D finite element for magneto-electro-elastic generally layered beam is presented. The model for the smart laminated beams is based upon the Timoshenko's beam theory [15], to take into account shear deformation effects. The electro-magnetic state is assumed as quasi-static and no electric charge and current density inside the beam are considered. The analytical model of the beam is presented in section 2 while the finite element model is derived in section 3. Last, numerical results are presented in section 4 to validate the finite element model and to show the potentiality of the proposed 1-D FEM for magneto-electro-elastic structures.

# 2 MEE beam model

Let us consider a straight beam lying in the $x - z$ plane, as shown in Figure 1. The beam has length $L$ and rectangular cross-section of unitary width and height $h$. The beam is realized by stacking $N$ magneto-electro-elastic layers, that are assumed to be perfectly bonded, with poling direction parallel to the $z$ axis. The faces of the $k - th$ layer are located at $z = h_{k-1}$ and $z = h_k$. Based on the Timoshenko's beam theory [15] for taking into account shear strain effect, the following kinematical model holds

$$\begin{aligned} u(x, z, t) &= u_0(x, t) - z\vartheta(x, t) \\ w(x, z, t) &= w_0(x, t) \end{aligned} \tag{1}$$

where $u$ and $w$ are the axial and transverse displacements of a point belonging to the beam while $u_0$ and $w_0$ are the axial and transverse displacements of beam axis points and $\theta$ is the cross-sectional rotation whereas $t$ denotes the time. The magneto-electric state of the beam is assumed to be quasistatic and is described in terms of

scalar electrical and magnetic potentials functions, $\varphi$ and $\psi$ respectively, as no charge density and current density are considered inside each layer. Moreover, the in-plane electric and magnetic fields components, $E_x$ and $H_x$, are considered negligible[16] with respect to the transverse ones, $E_z$ and $H_z$, which are related to the scalar potential functions by the gradient relationships

$$E_z = -\frac{\partial \varphi}{\partial z}, \quad H_z = -\frac{\partial \psi}{\partial z}. \tag{2}$$

The stress components $\sigma_{xx}$ and $\sigma_{xz}$ involved into the analysis as well as the electric displacement components, $D_x$ and $D_z$, and the magnetic inductions ones, $B_x$ and $B_z$, are obtained from the reduced constitutive relationships[14] that, for the $k-th$ layer, states

$$\begin{aligned}
\sigma_{xx}^{\langle k \rangle} &= c^{\langle k \rangle}(\frac{\partial u_0}{\partial x} - z\frac{\partial \vartheta}{\partial x}) - e^{\langle k \rangle} E_z^{\langle k \rangle} - d^{\langle k \rangle} H_z^{\langle k \rangle} \\
\sigma_{xz}^{\langle k \rangle} &= c_{55}^{\langle k \rangle}(\frac{\partial w_0}{\partial x} - \vartheta) \\
D_x^{\langle k \rangle} &= e_{15}^{\langle k \rangle}(\frac{\partial w_0}{\partial x} - \vartheta) \\
D_z^{\langle k \rangle} &= e^{\langle k \rangle}(\frac{\partial u_0}{\partial x} - z\frac{\partial \vartheta}{\partial x}) + \varepsilon^{\langle k \rangle} E_z^{\langle k \rangle} + \eta^{\langle k \rangle} H_z^{\langle k \rangle} \\
B_x^{\langle k \rangle} &= d_{15}^{\langle k \rangle}(\frac{\partial w_0}{\partial x} - \vartheta) \\
B_z^{\langle k \rangle} &= d^{\langle k \rangle}(\frac{\partial u_0}{\partial x} - z\frac{\partial \vartheta}{\partial x}) + \eta^{\langle k \rangle} E_z^{\langle k \rangle} + \mu^{\langle k \rangle} H_z^{\langle k \rangle}
\end{aligned} \tag{3}$$

where the notation $*^{\langle k \rangle}$ is used to label quantities pertaining to $k-th$ layer, $c$ and $c_{55}$ represent elastic stiffness constants, $e$ and $e_{15}$ are the piezoelectric constants, $d$ and $d_{15}$ are the piezomagnetic coupling while $\varepsilon$ and $\mu$ are the dielectric constant and magnetic permeability, respectively. The last material constant $\eta$ represents the direct magneto-electric coupling characteristic which is nonzero only in magneto-electro-elastic composites.

The magneto-electric problem is solved first in terms of mechanical primary variables by integrating the Gauss' laws for electrostatic and magnetostatic

$$\frac{\partial D_x}{\partial x} + \frac{\partial D_z}{\partial z} = 0, \qquad \frac{\partial B_x}{\partial x} + \frac{\partial B_z}{\partial z} = 0. \tag{4}$$

and taking into account both the electric and magnetic interface continuity conditions

$$\varphi^{\langle k \rangle}(x, h_k, t) = \varphi^{\langle k+1 \rangle}(x, h_k, t), \qquad D_z^{\langle k \rangle}(x, h_k, t) = D_z^{\langle k+1 \rangle}(x, h_k, t) \tag{5}$$

$$\psi^{\langle k \rangle}(x, h_k, t) = \psi^{\langle k+1 \rangle}(x, h_k, t), \qquad B_z^{\langle k \rangle}(x, h_k, t) = B_z^{\langle k+1 \rangle}(x, h_k, t) \tag{6}$$

as well as the following magneto-electric boundary conditions

$$\varphi(x, -h/2, t) = \xi_1, \qquad \varphi(x, h/2, t) = \xi_3 \tag{7}$$

$$\psi(x, -h/2, t) = \xi_2, \qquad \psi(x, h/2, t) = \xi_4 \tag{8}$$

It is obtained that the electric and magnetic potentials write as

$$\varphi^{\langle k\rangle}(x,z,t) = \zeta_{\varphi u}^{\langle k\rangle}(z)\,\frac{\partial u_0}{\partial x} + \zeta_{\varphi\vartheta}^{\langle k\rangle}(z)\,\frac{\partial \vartheta}{\partial x} + \zeta_{\varphi w}^{\langle k\rangle}(z)\,\frac{\partial^2 w_0}{\partial x^2} + \sum_{i=1}^{4}\zeta_{\varphi\xi_i}^{\langle k\rangle}(z)\,\xi_i \tag{9}$$

$$\psi^{\langle k\rangle}(x,z,t) = \zeta_{\psi u}^{\langle k\rangle}(z)\,\frac{\partial u_0}{\partial x} + \zeta_{\psi\vartheta}^{\langle k\rangle}(z)\,\frac{\partial \vartheta}{\partial x} + \zeta_{\psi w}^{\langle k\rangle}(z)\,\frac{\partial^2 w_0}{\partial x^2} + \sum_{i=1}^{4}\zeta_{\psi\xi_i}^{\langle k\rangle}(z)\,\xi_i \tag{10}$$

where $\zeta_{\alpha\beta}$ are known function of transverse coordinate $z$. Thus, to obtain the complete distributions of the magneto-electric variables, the mechanical equilibrium problem is to be addressed. The resultant axial $P$ and shearing $V$ forces as well as the bending moment $M$ are then introduced

$$P = K_{Pu}\frac{\partial u_0}{\partial x} + K_{P\vartheta}\frac{\partial \vartheta}{\partial x} + K_{Pw}\frac{\partial^2 w_0}{\partial x^2} + \sum_{i=1}^{4}K_{P\xi_i}\xi_i \tag{11}$$

$$V = K_V(\frac{\partial w_0}{\partial x} - \vartheta) \tag{12}$$

$$M = K_{Mu}\frac{\partial u_0}{\partial x} + K_{M\vartheta}\frac{\partial \vartheta}{\partial x} + K_{Mw}\frac{\partial^2 w_0}{\partial x^2} + \sum_{i=1}^{4}K_{M\xi_i}\xi_i \tag{13}$$

where $K_{\alpha\beta}$ are the effective stiffness coefficients of the smart laminated beam obtained by integrating over the beam height the stress components in light of the constitutive relationships Equations (3) and of the electric and magnetic potential functions Equations (9). The beam stress resultants are then involved in the following equilibrium equations

$$\frac{\partial P}{\partial x} + p_x = I_0\frac{\partial^2 u_0}{\partial t^2} + I_1\frac{\partial^2 \vartheta}{\partial t^2} \tag{14}$$

$$\frac{\partial V}{\partial x} + p_z = I_0\frac{\partial^2 w_0}{\partial t^2} \tag{15}$$

$$\frac{\partial M}{\partial x} + V + m = I_1\frac{\partial^2 u_0}{\partial x^2} + I_2\frac{\partial^2 \vartheta}{\partial x^2} \tag{16}$$

where $I_i$ are the inertia terms while $p_x$ and $p_z$ are axial and transverse force distributed over the beam span while $m$ represents externally applied distributed bending moment. By substituting the stress resultants definition Equations (11) to (13) into the equilibrium Equations (14) to (16) the governing equations of motion of the laminated magneto-electro-elastic beam are obtained.

# 3 Finite Element Formulation

In order to write down the finite element formulation of the developed multi-layer piezoelectromagnetic beam, the shape functions are first derived in such a way the approximated displacement field fulfills the equations of motion in homogeneous form.

These are obtained by enforcing to zero both the mechanical distributed loads and the electro-magnetic boundary conditions $\xi_i$. By integrating the homogenous shear equilibrium Equation (15) written in terms of kinematical variables through the shear force definition Equation (12), the following relationship that allows to write the cross-sectional rotation $\vartheta$ in terms of the transverse displacement $w_0$ is found

$$\vartheta(x) = \frac{\partial w_0}{\partial x} + C \tag{17}$$

where $C$ is an integration constant to be determined as follows. By substituting Equation (17) into the axial homogenous equilibrium Equation (14) written in terms of the beam mean-line displacement variables via Equation (11), the in-plane displacement $u_0$ is related to the transverse one $w_0$ by the differential equation

$$\frac{\partial^2 u_0}{\partial x^2} = -b\frac{\partial^3 w_0}{\partial x^3} \tag{18}$$

that is used together with Equation (17) into Equation (16) along with the bending moment Equation (13) and the shear force Equation (12) definitions to get the integration constant as

$$C = a\frac{\partial^3 w_0}{\partial x^3} \tag{19}$$

where the coefficients $a$ and $b$ in the preceding formulas are adequately defined in terms of the beam equivalent stiffness characteristics $K_{\alpha\beta}$

By integrating twice Equation (18) it is found that the mean-line axial displacement can be approximated by using a linear interpolation function in addition to the transverse displacement derivative contribution

$$u_0 = A_1 + A_2 x - b\frac{\partial w_0}{\partial x} \tag{20}$$

moreover a third order interpolation function is selected to represent the transverse displacement function as

$$w_0 = A_3 + A_4 x + A_5 x^2 + A_6 x^3 \tag{21}$$

which also allows to write the cross-sectional rotation as a second order polynomial in light of Equation (17) and (19).

In a more compact form, the generalized displacement variables are collected in a vector $\mathbf{U}(x)=\left[\begin{array}{ccc} u_0(x) & w_0(x) & \theta(x) \end{array}\right]^T$ and their approximated representation is written in matrix form as

$$\mathbf{U}(x) = \mathbf{\Phi}(x)\,\mathbf{A} \tag{22}$$

where $\mathbf{A}$ collects the interpolation coefficients $A_i,\ i = 1, .., 6$ while $\mathbf{\Phi}$ is the interpolation matrix. To obtain the matrix of shape functions, the interpolation coefficients $\mathbf{A}$ are written in terms of nodal displacement $\mathbf{\Delta_e} = \left[\begin{array}{cc} \mathbf{U}^T(x_i) & \mathbf{U}^T(x_j) \end{array}\right]^T$ by writing Equation (22) to the first $i$ and second $j$ node of the beam finite element, it follows

that $\mathbf{A} = \bar{\bar{\mathbf{\Phi}}}^{-1}\mathbf{\Delta_e}$ being $\bar{\bar{\mathbf{\Phi}}}$ the interpolation matrix collocated to the nodal points and thus, from Equation (22),

$$\mathbf{U}(x,t) = \mathbf{N}(x)\mathbf{\Delta_e}(t) \tag{23}$$

being $\mathbf{N}$ the matrix of shape functions defined as

$$\mathbf{N}(x) = \mathbf{\Phi}(x)\bar{\bar{\mathbf{\Phi}}}^{-1} \tag{24}$$

At this point, to obtain the weak form of the equations of motion, the equilibrium Equations (14)- (16) are multiplied by the virtual displacement components $\delta u_0$, $\delta w_0$ and $\delta\vartheta$, are integrated over the element length and are expressed in term of kinematical variables vie the stress resultants definitions Equations (11)- (13). In a compact matrix form they write as

$$\begin{aligned}\int_L \frac{\partial}{\partial x}\left(\delta\mathbf{U}^T\right)\,\mathcal{D}_M\left(\mathbf{U}\right)dx - \int_L \delta\mathbf{U}^T\mathcal{D}_V\left(\mathbf{U}\right)dx + \int_L \delta\mathbf{U}^T\,\mathbf{I}\,\frac{\partial^2}{\partial t^2}\left(\mathbf{U}\right)dx = \\ \int_L \delta\mathbf{U}^T\,\mathbf{f}dx - \int_L \frac{\partial}{\partial x}\left(\delta\mathbf{U}^T\right)\,\mathbf{F}_{EM}dx + \left[\delta\mathbf{U}^T\,\bar{\mathbf{F}}\right]_0^L\end{aligned} \tag{25}$$

where $\mathcal{D}_\mathcal{M}$ and $\mathcal{D}_\mathcal{V}$ are adequately defined operator and $\mathbf{I}$ is the matrix containing inertia contributions. In Equations (25) $\bar{\mathbf{F}} = \left\{\bar{P} \quad \bar{V} \quad \bar{M}\right\}^T$ is the boundary forces vector, $\mathbf{f} = \left\{p_x \quad p_z \quad m\right\}^T$ collects the distributed mechanical forces and moment per unit length, and $\mathbf{F}_{EM}$ is the vector containing the contribution of the boundary forces and moments generated by the electromagnetic boundary conditions $\xi_i$ and writes as

$$\mathbf{F}_{EM} = \sum_{i=1}^{4}\begin{Bmatrix} K_{P\xi_i} \\ 0 \\ K_{M\xi_i}\end{Bmatrix}\xi_i. \tag{26}$$

By using the displacement fields approximation Equation (23) into Equation (25), the discrete elemental equilibrium equations are obtained

$$\mathbf{M}\ddot{\mathbf{\Delta}}_\mathbf{e} + \mathbf{K}\mathbf{\Delta_e} = \mathbf{F}_{eq} \tag{27}$$

where dots are used to represent time derivatives, $\mathbf{M}$ is the element consistent mass matrix defined by Equation (28)

$$\mathbf{M} = \int_L \mathbf{N}^T\,\mathbf{I}\,\mathbf{N}dx \tag{28}$$

and $\mathbf{K}$ is the element stiffness matrix

$$\mathbf{K} = \int_L \frac{\partial}{\partial x}\left(\mathbf{N}^T\right)\,\mathcal{D}_M\left(\mathbf{N}\right)dx - \int_L \mathbf{N}^T\mathcal{D}_V\left(\mathbf{N}\right)dx \tag{29}$$

In particular, the mass matrix is full while the element stiffness has the following structure

$$\mathbf{K} = \begin{bmatrix} K_{11} & 0 & K_{13} & -K_{11} & 0 & -K_{13} \\ & K_{22} & K_{23} & 0 & -K_{22} & K_{23} \\ & & K_{33} & -K_{13} & -K_{23} & K_{36} \\ & & & K_{11} & 0 & K_{13} \\ & \textit{Symm} & & & K_{22} & -K_{23} \\ & & & & & K_{33} \end{bmatrix} \tag{30}$$

evidencing an inherent axil-bending coupling term $K_{13}$. The equivalent forces $\mathbf{F}_{eq}$ include the contribution of the nodal forces and of both mechanical and electro-magnetic loads distributed over the beam span

$$\mathbf{F}_{eq} = \mathbf{F}_N + \mathbf{F}_{eq,M} + \mathbf{F}_{eq,EM} \tag{31}$$

where

$$\mathbf{F}_N = \left[\mathbf{N}^T \bar{\mathbf{F}}\right]_0^L \tag{32}$$

$$\mathbf{F}_{eq,M} = \int_L \mathbf{N}^T \mathbf{f} dx \tag{33}$$

$$\mathbf{F}_{eq,EM} = -\int_L \frac{\partial}{\partial x}\left(\mathbf{N}^T\right) \mathbf{F}_{EM} dx \tag{34}$$

# 4 Numerical Results

The proposed finite element model is first validate by comparing results obtained for a single layer piezoelectric cantilever beam undergoing a through-the-thickness difference of electric potential $\Delta\varphi = 1\,V$ with 2-D plane stress results computed by using the commercial finite element code COMSOL Multiphysics©. The beam dimensions are $L = 0.3\,m$ and $h = 0.02\,m$ while material properties of the $BaTiO_3$ piezoelectric phase are reported in Table 1. Static simulations are first carried out using the

| $BaTiO_3$ | | | | |
|---|---|---|---|---|
| $C_{ij}[10^9 Pa]$ | $\varepsilon_{ij}[10^{-9}\frac{F}{m}]$ | $e_{ij}[\frac{C}{m^2}]$ | $\mu_{ij}[10^{-6}\frac{Ns^2}{C^2}]$ | $d_{ij}[\frac{NA}{m}]$ |
| $C_{11}$= 150.4 | $\varepsilon_{11}$=9.9 | $e_{31}$=-4.3 | $\mu_{11}$=5 | $d_{31}$=0 |
| $C_{33}$= 145.5 | $\varepsilon_{33}$=11.1 | $e_3$=17.4 | $\mu_{33}$=0 | $d_{33}$=0 |
| $C_{12}$= 65.6 | | $e_{15}$=11.4 | | $d_{15}$=0 |
| $C_{13}$= 65.9 | | | | |
| $C_{55}$= 43.9 | | | | |

Table 1: Piezoelectric material constants.

proposed 1-D FEM, with just one finite element, and the 2-D FEM model. Results for the axial displacement of the beam free end are found to be in good accordance, namely $u_0 = 1.17\,nm$ with a percentage error of about $0.8\%$. A mesh consisting of ten finite elements is then used to compute the natural frequencies of the beam, which

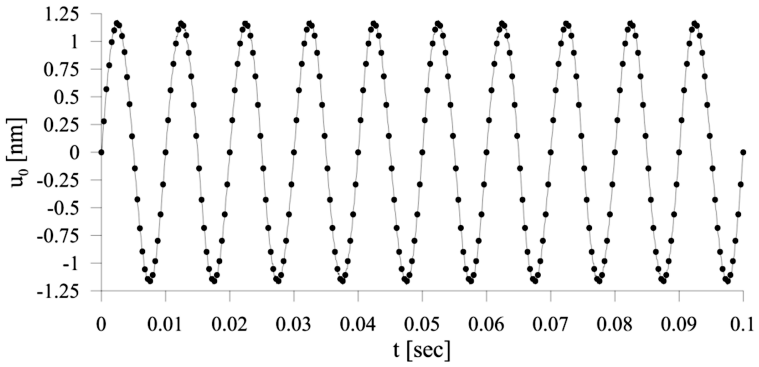


Figure 2: Comparison of the axial displacement of the piezoelectric beam undergoing electrical load.

are reported in Table 2 for the five lowest vibration modes in comparison with 2-D FEM calculation. Percentage discrepancy are also reported evidencing the soundness of the proposed finite element model. Transient results are also compared with 2-D

| mode | 1-D FEM | 2-D FEM | Error % |
|---|---|---|---|
| 1 | 160.76 | 160.81 | 0.03 |
| 2 | 987.99 | 989.13 | 0.11 |
| 3 | 2689 | 2692.94 | 0.15 |
| 4 | 3665 | 3662.94 | 0.06 |
| 5 | 5084.2 | 5083.17 | 0.02 |

Table 2: Natural frequencies [Hz] of the clamped-free piezoelectric beam.

FEM calculations and good agreement is found. The applied difference of electric potential is let vary sinusoidally at 100 Hz. Under such electrical input the piezoelectric bar extends and contracts as it stems from the time history of the beam free end axial displacement shown in Fig. 2

The second validation analysis deals with a bimorph piezoelectric-piezomagnetic layered beam. The beam length is $L = 0.3\,m$ while each layer is $0.01\,m$ thick. The electric potential as well as the magnetic one are set to zero on both the bottom and top surface of the beam. The material constant for the piezoelectric barium titanate layer and the piezomagnetic cobalt ferrite material are taken from reference [17] and are not reported here for the sake of conciseness. Natural frequencies of the beam under distinct boundary conditions are computed using the present 1-D FEM and are reported in Table 3 in comparison with plane stress 2-D FEM results available in literature [17]. The considered boundary conditions configurations are the clamped-clamped one, C-C, the cantilever configuration, referred to as C-F, and the simply-supported one, named S-S. Good agreement has been found for the natural frequencies up to the tenth vibrational mode regardless of the mechanical boundary conditions.

Last a piezoelectric-piezomagnetic frame structure is analyzed with the aim of

| | C-C | | C-F | | S-S | |
|---|---|---|---|---|---|---|
| mode | present | 2-D FEM [17] | present | 2-D FEM [17] | present | 2-D FEM [17] |
| 1 | 1156.58 | 1167.56 | 187.74 | 189.63 | 524.50 | 529.80 |
| 2 | 3053.00 | 3080.24 | 1148.21 | 1159.42 | 2044.82 | 2065.44 |
| 3 | 5683.13 | 5730.43 | 3100.11 | 3129.14 | 4356.68 | 4420.84 |
| 4 | 8837.19 | 8841.68 | 4420.87 | 4420.84 | 4486.12 | 4467.87 |
| 5 | 8871.80 | 8935.91 | 5790.68 | 5841.67 | 7496.08 | 7561.09 |
| 6 | 12467.01 | 12555.58 | 9061.09 | 9136.27 | 11080.17 | 11174.64 |
| 7 | 16373.38 | 16479.50 | 12761.99 | 12861.96 | 13251.23 | 13262.52 |
| 8 | 17681.75 | 17683.36 | 13263.48 | 13262.52 | 15056.09 | 15165.55 |
| 9 | 20507.02 | 20626.50 | 16779.44 | 16897.13 | 19287.60 | 19423.23 |
| 10 | 24807.48 | 24937.25 | 21017.64 | 21155.73 | 22085.52 | 22104.20 |

Table 3: Natural frequencies [Hz] response of the magnetoelectric bimorph.

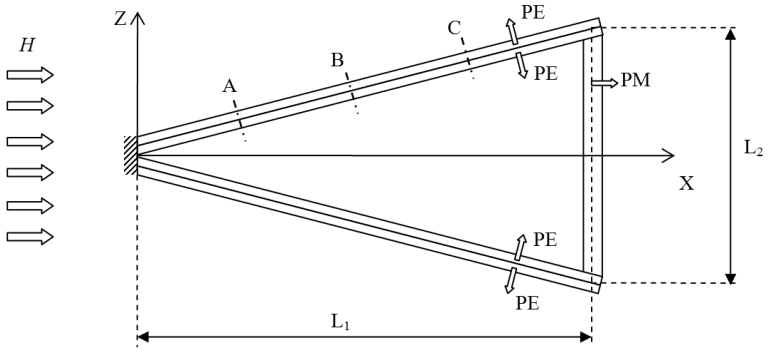


Figure 3: Magneto-electro-elastic frame structure.

showing the versatility of the proposed formulation in analyzing complex magneto-electro-elastic structures. The frame consists of two piezoelectric bimorph in series arrangement which share the clamped ends while they are connected by a piezomagnetic bar at the opposite ends, as shown in Fig.3, where the electric poling and the magnetization direction are schematically shown by the PE and PM arrows, respectively. The piezoelectric bimorph layers are $1\,mm$ thick while the thickness of the piezomagnetic bar is $2\,mm$. With reference to Fig.3, the frame overall dimensions are $L_1 = 1\,cm$ and $L_2 = 5\,mm$. Materials properties for the piezoelectric PZT-5A and the piezomagnetic $CoFe_2O_4$ are reported in Table 4 and 5, respectively. The mass density of the piezoelectric layer is $\rho = 7750\,kg/m^3$ while that of the cobalt ferrite is $\rho = 5300\,kg/m^3$.

PZT-5A

| $C_{ij}[10^9 Pa]$ | $\varepsilon_{ij}[10^{-9}\frac{F}{m}]$ | $e_{ij}[\frac{C}{m^2}]$ | $\mu_{ij}[10^{-6}\frac{Ns^2}{C^2}]$ | $d_{ij}[\frac{NA}{m}]$ |
|---|---|---|---|---|
| $C_{11}$= 120.3 | $\varepsilon_{11}$=8.14 | $e_{31}$=-5.4 | $\mu_{11}$=5 | $d_{31}$=0 |
| $C_{33}$= 110.9 | $\varepsilon_{33}$=7.32 | $e_{3}$=15.8 | $\mu_{33}$=0 | $d_{33}$=0 |
| $C_{12}$= 75.1 | | $e_{15}$=12.3 | | $d_{15}$=0 |
| $C_{13}$= 75.2 | | | | |
| $C_{55}$= 21.1 | | | | |

Table 4: Piezoelectric material constants.

| $CoFe_2O_4$ | | | | |
|---|---|---|---|---|
| $C_{ij}[10^9 Pa]$ | $\varepsilon_{ij}[10^{-9}\frac{F}{m}]$ | $e_{ij}[\frac{C}{m^2}]$ | $\mu_{ij}[10^{-6}\frac{Ns^2}{C^2}]$ | $d_{ij}[\frac{NA}{m}]$ |
| $C_{11}$= 286 | $\varepsilon_{11}$=0.08 | $e_{31}$=0 | $\mu_{11}$=-590 | $d_{31}$=580.3 |
| $C_{33}$= 269.5 | $\varepsilon_{33}$=0.093 | $e_{33}$=0 | $\mu_{33}$=157 | $d_{33}$=699.7 |
| $C_{12}$= 170.5 | | $e_{15}$=0 | | $d_{15}$=550 |
| $C_{13}$= 173 | | | | |
| $C_{55}$= 45.3 | | | | |

Table 5: Piezomagnetic material constants.

The structure undergoes a magnetic field $H = 5\,Oe$ which applies to the piezomagnetic bar as a through-the-thickness difference of magnetic potential $\Delta\psi = 0.12566\,mA$. Under static magnetic field the structure deforms as shown in Fig.4, where the through-the-thickness distributions of the electric potential in the piezoelectric bimorph are also drawn for section A at $(X = L/4)$, B at $(X = L/2)$ and C at $(X = 3L/4)$. The

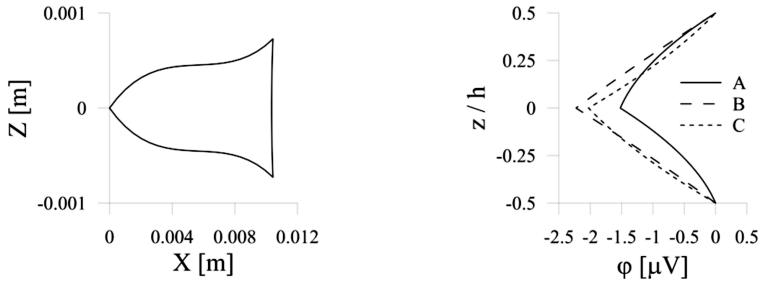


Figure 4: Left, structure deformation under DC magnetic field. Right, electric potential distribution in the PZT-5A beam.

natural vibration response is then computed and it is shown in Fig.5. The modal shapes corresponding to the six lowest natural frequencies are plotted evidencing symmetric and asymmetric vibrational modes. Last, the frequency response of the magneto-electro-elastic frame structure is studied. An AC magnetic field maintained at 5 Oe is applied and the excitation frequency $f$ is let vary from $0$ to $120\,kHz$. The response of the structure is shown in Fig.6 in terms of the electric potential read at the bimorph layer interface at the three considered sections. Although the excitation frequency range involves the six lowest natural frequencies, resonance peaks are related only to the second, the fourth and sixth vibrational modes.

# 5 Conclusion

A two-node finite element for one-dimensional magneto-electro-elastic beams, which enables the modelling of generally layered magneto-electro-elastic structures, has been presented. An elastic equivalent single-layer representation of the multi-field multilayered problem is first obtained by condensing the electro-magnetic state of the beam to the mechanical variables. The proposed finite element is characterized by

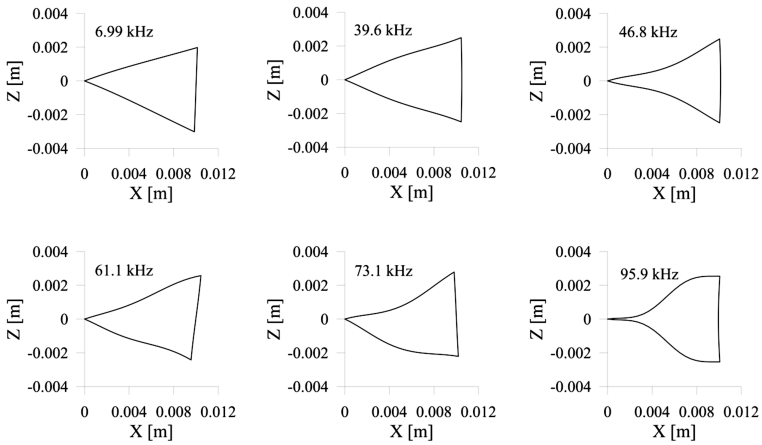


Figure 5: Natural frequencies and modal shapes.

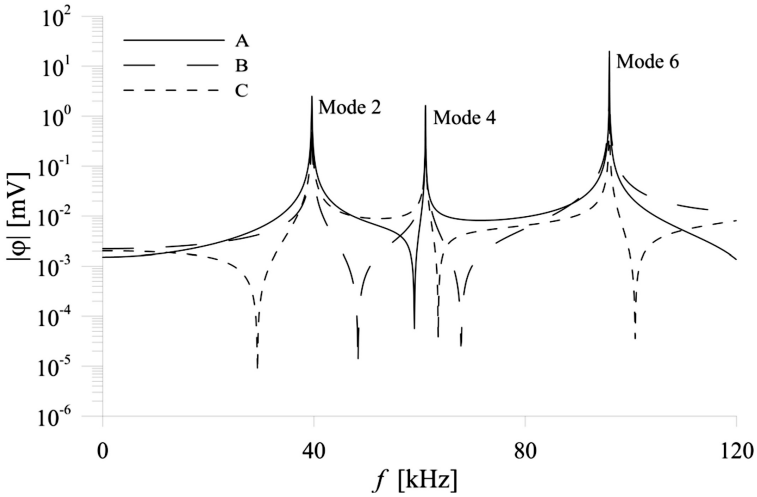


Figure 6: Frequency response of the magneto-electro-elastic structure.

three degrees of freedom per nodes, *i.e.* the longitudinal and transverse displacement components and the cross-sectional rotation, and the electro-magnetic state characterization constitutes a post-processing step. It follows that this one-dimensional finite element for magneto-electro-elastic layered structures can be easily implemented in any existing computer code based on the Bernoulli beam finite element. Numerical results have been presented proving the soundness of the finite element model developed.

# References


[1] M. Fiebig, "Revival of the magnetoelectric effect", Journal of Physics D: Applied Physics, 38, R123-152, 2005.

[2] C. W. Nan, "Magnetoelectric effect in composite of piezoelectric and piezomagnetic phase", Physics Review B, 50, 6082-6088, 1994.

[3] J. Ryu and S. Priya and K. Uchino and H-E. Kim, "Magnetoelectric Effect in Composites of Magnetostrictive and Piezoelectric Materials", Journal of Electroceramics, 8(2), 107-119, 2002.

[4] A. Bayrashev and W.P. Robbins and B. Ziaie, "Low frequency wirelwss powering of Microsystems using piezoelectric-magnetostrictive laminate composites", Sensors and Actuators A, 114, 244-249, 2004.

[5] T.L. Wu and J.H. Huang, "Closed-form solutions for the magnetoelectric coupling coefficients in fibrous composites with piezoelectric and piezomagnetic phases", International Journal of Solids and Structures, 37, 2981-3009, 2000.

[6] J. Zhai and Z. Xing and S. Dong and J. Li and D. Viehland, "Detection of pico-Tesla magnetic fields using magneto-electric sensors at room temperature", Applied Physics Letters, 88, 062510(3), 2006.

[7] L. Bian and Y. Wen and P. Li and Q. Gao and M. Zheng, "Magnetoelectric transducer with high quality factor for wireless power receiving", Sensors and Actuators A, 150, 207-211, 2009.

[8] A. Daga, N. Ganesan, K. Shankar, "Behaviour of magneto-electro-elastic sensors under transient mechanical loading", Sensors and Actuators A, 150, 46-55, 2009.

[9] E. Pan, P.R. Heyliger, "Free vibrations of simply supported and multilayered magneto-electro-elastic plates", Journal of Sound and Vibration, 252(3), 429-442, 2002.

[10] D.J. Huang, H.J. Ding, W.Q. Chen, "Analytical solution for functionally graded magneto-electro-elastic plane beams", International Journal of Engineering Science, 45, 467-485, 2007.

[11] C.P. Wu, Y.C. Lu, "A modified Pagano method for the 3D dynamic responses of functionally graded magneto-electro-elastic plates", Composite Structures, 90, 363-372, 2009.

[12] J.M. Simões Moita, C.M. Mota Soares, C.A. Mota Soares "Analyses of magneto-electro-elastic plates using a higher finite element model", Composite Structures, 91, 421-426, 2009.

[13] A. Milazzo, I. Benedetti, C. Orlando, "Boundary element method for magneto-electro-elastic laminates", Computer Modeling in Engineering and Sciences, 15(1), 17-30, 2006.

[14] A. Milazzo, C. Orlando, A. Alaimo, "An analytical solution for the magneto-electro-elastic bimorph beam forced vibrations problem", Smart Materials and Structures, 18, 085012 (14 pp) , 2009.

[15] Timoshenko S "Vibration problems in engineering" Princeton: D. Van Nostrand Company, Inc. 1955

[16] Liu MF "An exact deformation analysis for the magneto-electro-elastic fiber-

reinforced thin plate" Applied Mathematical Modelling, 35, 2443-2461, 2011
[17] A.R. Annigeri, N. Ganesan, S. Swarnamani, "Free vibration behaviour of multiphase and layered magneto-electro-elastic beam", Journal of Sound and Vibration, 299, 44-63, 2007.